RADAR BACKSCATTER FROM THE OCEAN: DEPENDENCE ON SURFACE FRICTION VELOCITY

W. LINWOOD JONES and L. C. SCHROEDER
NASA Langley Research Center, Hampton, Virg., U.S.A.

(Received 4 November, 1977)

Abstract. From the mid 1960s to the present, the normalized radar cross-section (NRCS) of the ocean has been measured using airborne radars operating over a frequency range of 0.4 to 14 GHz. Analyses of these data have shown that the NRCS was proportional to the ocean surface wind speed raised to some power, but the values of the exponent remained in dispute. This paper extends previous work and uses these NRCS measurements to demonstrate that to the first order, the NRCS is a function of only the friction velocity at the ocean's surface. Further analyses characterize the dependence of the NRCS on radar variables such as frequency, incidence angle, polarization, etc. Finally, recommendations are made for using Ku-band radars at large incidence angles for remote sensing of the wind friction velocity vector.

1. Introduction

For many years, the radar scattering properties of the ocean have been a popular topic of research for radio scientists. From an analytical viewpoint, the ocean is attractive because its roughness can be described by statistical methods and the scattering problems are in principle tractable. From a practical viewpoint, the ocean's scattering signature, normalized radar cross-section (NRCS) or σ° vs incidence angle, holds promise for remote sensing of valuable surface variables such as wind speed and direction. Early experiments by Cowan (1946), Kerr (1951) and Grant and Yapley (1957), demonstrated that the NRCS was dependent on ocean surface winds. From 1965 to 1971, personnel of the Naval Research Laboratory (NRL) made aircraft measurements (Daley *et al.*, 1968, 1970, 1971, 1973a) to determine the relationship between NRCS and ocean surface conditions. Later, other aircraft measurements were obtained by personnel of the National Aeronautics and Space Administration (NASA) and reported by Krishen (1971), Bradley (1971), Newton and Rouse (1972), Claassen *et al.* (1972a) and Jones *et al.* (1977). NASA also obtained the only satellite-borne microwave scatterometer measurements during the Skylab Experiment (June 1973 through February 1974).

The purpose of this paper is to extend previous work and use these data to characterize the dependence of the ocean scattering signature (for incidence angles between 30° and 60°) on the surface friction velocity U_*.

2. NRCS Measurements

2.1. NRL Flight Experiments

Perhaps the most extensive measurements of the radar sea return observed from aircraft were performed by personnel of the NRL during the period 1965 to 1971.

They used a four-frequency radar (4-FR) to measure the NRCS as a function of wind, significant ocean-wave height, and radar configuration: incidence angle, polarization and wavelength. The system was an airborne coherent-pulsed radar capable of transmitting and receiving a sequence of four frequencies: X-band (8.9 GHz), C-band (4.5 GHz), L-band (1.3 GHz), and P-band (0.43 GHz). The majority of the measurements were obtained during four major programs, viz., Puerto Rico (1965), North Atlantic (1969), Bermuda (1970, JOSS 1), and East Coast U.S. (1971, JOSS 2). A detailed listing for each flight giving the date and location, the major radar parameters and sea-surface conditions is given by Daley (1973b).

2.2. NASA JOHNSON SPACE CENTER FLIGHT EXPERIMENTS

From March 1966 through February 1971, the NASA Johnson Space Center (JSC) personnel investigated the application of a microwave scatterometer to measure surface winds over the ocean. Eight missions were conducted in the North Atlantic using aircraft instrumented with a 13.3-GHz fan-beam scatterometer. The scatterometer system was a continuous-wave, fan-antenna beam, Doppler radar designed to measure simultaneously the vertically-polarized NRCS over an incidence-angle range of $\pm 60°$. The last two missions (119 and 156) had the best 'surface truth'. Mission 119 corresponded to the JOSS 1 experiment and obtained wind speed and wind direction measurements from the U.S. Navy 'Argus Island' tower located approximately 15 km southwest of Bermuda. Mission 156 corresponded to JOSS 2 and obtained wind measurements from the National Oceanographic and Atmospheric Administration (NOAA) buoy XERB-1 and the weather ships *Hotel* and *Range Recoverer.*

2.3. NASA LANGLEY RESEARCH CENTER FLIGHT EXPERIMENTS

From 1973 to the present, a 13.9GHz aircraft 'pencil-beam' microwave scatterometer (AAFE RADSCAT) was used by personnel from the NASA Langley Research Center (LaRC) to obtain ocean NRCS measurements for vertical and horizontal polarizations as a function of incidence angle and azimuth angle relative to surface wind direction. Measurements were obtained over open oceans for a variety of surface conditions from light winds and calm seas to gales. For each flight, the local ocean-surface wind speed and wave conditions were either measured by surface instruments or by aircraft.

2.4. SKYLAB S-193 SATELLITE EXPERIMENT

The only satellite ocean NRCS measurements were obtained from the NASA Skylab earth resources experiment. The instrument used was a mechanically scanned 'pencil-beam', 13.9-GHz combination *rad*iometer/*scat*terometer (similar to AAFE RADSCAT) known as the S-193 RADSCAT. Data were taken during the Skylab 2, 3, and 4 missions from June 1973 through February 1974. During this time, 82 data segments partially or completely over water were recorded. Many of the segments had little useful oceanographic data; nevertheless, a substantial amount of NRCS data is available for wind speeds from 2.5 to 30 m s^{-1} and for latitudes ranging from the tropics to 50° N. Measurements were also obtained near the eye of hurricane Ava and the tropical storm Christine. A detailed listing of each data segment giving the orbit, date, location, and RADSCAT mode is given by Cardone *et al.* (1975) and Young and Moore (1977).

3. NRCS/Ocean-Surface-Conditions Analyses

3.1. NRCS VS WIND SPEED

An empirical power-law relationship between the NRCS and wind speed has been suggested by Guinard *et al.* (1971) and Bradley (1971):

$$\sigma^\circ = aU^\chi \,, \tag{1}$$

where a is a constant, U is the observed wind speed, and χ is the wind-speed exponent. An alternate form is obtained by taking the base-ten logarithm and multiplying by ten, which yields

$$\sigma^\circ(\text{dB}) = a(\text{dB}) + \chi(10 \log U) \,, \tag{2}$$

where (dB) denotes decibels.

3.1.1. *NRL 4-FR Data*

Daley Analysis. – Daley (1973b, c), performed a regression analysis using Equation (1) to relate the NRCS to wind speed for upwind (radar looking into wind), downwind, and crosswind observations. His analysis used the measurements from all NRL aircraft missions for depression angles (90° minus incidence angle) of 5° to 90° and for each frequency and polarization. For L- and P-bands, all data for $U > 0.5$ m s^{-1} were used; for the more wind-sensitive frequencies, X- and C-bands, only data for $U > 5$ m s^{-1} were used. The results are summarized in Table I.

TABLE I
Summary of wind-speed exponents for NRL 4-FR at incidence angles from 30 to 70°

Pol.	0.428 GHz	1.228 GHz	4.455 GHz	8.910 GHz
V	−0.3 to 0.2	−0.3 to 0.5	0.3 to 1.2	0.3 to 1.2
H	−0.1 to 0.5	−0.2 to 0.7	0.2 to 1.4	0.6 to 1.8

Claassen et al. Analysis. – An independent analysis of the NRL C-band and X-band data from the North Atlantic and JOSS 1 missions by Claassen *et al* (1972a, b) suggested a stronger wind dependence than reported by Daley (1973b, c). In this study, regression analyses using Equation (2), performed for each mission separately, uncovered what was believed to be systematic biases between missions.

An example of their analysis for X-band data is shown in Figure 1. Generally larger biases were observed for VV polarized data than were observed for HH polarized data, and similar biases were observed when similarly polarized upwind and downwind data were compared. Also similar trends were found in the C-band data although the biases were smaller. No satisfactory explanation for the biases in the X-band or C-band wind responses was readily apparent (see Jackson, 1974; Daley, 1974; Sittrop, 1974).

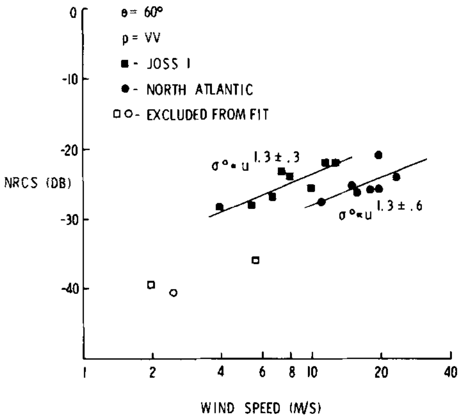

Fig. 1. Power law analysis of NRL 4-FR 8.9-GHz upwind data by mission. From Claassen (1972b).

To estimate the wind-speed response for the combined data set, the upwind and downwind biases were averaged in Claassen's analysis and then added to the North Atlantic data for each incidence angle. After the adjusted data (North Atlantic) were then combined with the JOSS 1 data, the regression analysis was again performed. The results for the combined-data-set were essentially the same as that for the individual missions. These results are summarized in Table II.

TABLE II

Wind-speed exponents: Claassen *et al.* analysis of NRL 4-FR North Atlantic (1969) and JOSS 1 (1970) NRCS data

Direction	Pol.	Incidence angle								
		30°		45°		60°		70°		
		4.5	8.9	4.5	8.9	4.5	8.9	4.5	8.9	Freq., GHz
Upwind	V	1.20	1.10	1.50	0.90	1.30	1.35	1.15	1.25	
	H	1.30	1.20	1.45	1.05	1.50	1.45	1.35	1.35	
Downwind	V	1.00	1.40	1.40	1.30	1.10	1.05	1.20	0.90	
	H	0.90	1.30	1.80	1.20	1.60	1.75	1.40	1.70	

Present analysis. – Because the Claassen *et al.* study applies only to the 4-FR X-band and C-band data, we extended their work to include the L-band and P-band data. Our analysis also uses Equation (2) and the same aircraft missions separately, but it is limited to only the 30-deg incidence data for all frequencies (X-band and C-band repeated for consistency of results). The North Atlantic and JOSS 1 data sets were from Daley (1970, 1971), respectively. All data except a 2.5 m s^{-1} wind-speed point for the North Atlantic were used. Again the wind-speed exponents are higher than reported by Daley. If the 2.5 m s^{-1} point were included, the wind-speed exponent would be similar to those reported by Daley. However, since the radar backscatter is known to decrease rapidly below a threshold wind speed of approximately 3.5 m s^{-1} (Cardone *et al.*, 1975, Chapter 6), the exclusion of the 2.5 m s^{-1} point is justified. The results of the wind-speed analysis are summarized in Table III.

TABLE III

Wind-speed exponents for 30° incidence from present analysis of NRL 4-FR data

(a) North Atlantic (1969)					
Direction	Pol.	Frequency, GHz			
		0.428	1.228	4.455	8.910
Upwind	V	0.69	1.47	0.91	0.95
	H	0.97	1.12	1.40	0.95
Downwind	V	0.34	1.12	0.55	1.19
	H	0.42	0.51	0.79	1.27
Crosswind	V	−0.26	1.01	1.57	2.06
	H	−0.10	0.64	1.04	1.55

(b) JOSS I (1970)					
Direction	Pol.	Frequency, GHz			
		0.428	1.228	4.455	8.910
Upwind	V	0.34	0.55	1.28	1.20
	H	0.47	1.54	1.35	0.70
Downwind	V	0.47	0.56	0.99	1.29
	H	0.96	0.74	1.35	1.08
Crosswind	V	0.58	0.23	1.31	1.22
	H	0.59	0.38	1.24	1.11

3.1.2. *NASA JSC* 13.3 *GHz Data*

Bradley (1971) analyzed the 13.3 GHz scatterometer data (upwind and crosswind) from Missions 119 and 156 using Equation (2) and subject to the condition that the

NRCS at any incidence angle be normalized to the NRCS value at an angle of 10 deg. Claassen (1972a) reexamined the 13.3-GHz data from mission 119 and 156 and added mission 88, using different statistical procedures for upwind, downwind, crosswind, and 45-deg diagonal-wind cases. The combined data from missions 88 and 119 and the data from mission 156 produced two power-law responses with nearly identical slopes but separated by a bias. The bias was believed to be the result of changes in the antenna pattern when the scatterometer was installed on a different aircraft for mission 156. Typical combined data for the three missions and the 'best fit' power law are shown in Figure 2. The wind-speed exponents were larger than reported by Daley but are comparable with the results of Claassen's analysis for 4-FR X-band. The exponents increase with incidence angle and have a weak dependence on wind direction. Upwind and downwind slopes are nearly equal while the crosswind value is slightly less. The wind-speed exponents from Bradley and Claassen are summarized in Table IV.

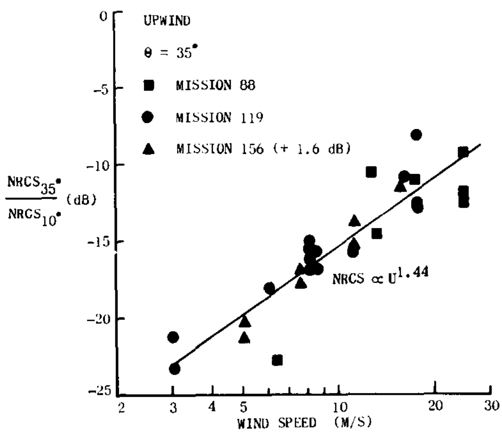

Fig. 2. Wind-speed dependence of 13.3-GHz NRCS at $\theta = 35°$ (Private communication, Claassen).

TABLE IV

Wind-speed exponents for 13.3 GHz Scatterometer at vertical polarization

Direction	Incidence angle			
	25°		35°	
	Bradley	Claassen	Bradley	Claassen
Upwind	1.12	1.10	1.49	1.42
Downwind	0.75	1.18	1.26	1.56
Crosswind		1.00		1.38
Upwind 45° diagonal		1.32		1.37
Downwind 45° diagonal		1.10		1.50

3.1.3. *NASA LaRC AAFE RADSCAT Data*

Jones *et al.* (1977) analyzed the AAFE RADSCAT NRCS measurements using Equation (2) and a 'neutral-stability' wind speed at a height of 19.5 m. The neutral-stability wind speed is defined as the wind speed that would result from a logarithmic wind-height relationship in a neutrally-stratified atmosphere. Unlike the NRL 4-FR and the 13.3-GHz data, no arbitrary biases were added to the AAFE RADSCAT NRCS measurements before comparison with wind speed. The wind-speed exponents were determined for upwind, downwind, and crosswind radar observations as a function of incidence angle and polarization and are summarized in Table V. These exponents are greater than those from Daley's analysis of the 4-FR data, but they are comparable with the 13.3-GHz scatterometer values.

TABLE V
Wind-speed exponents for 13.9 GHz AAFE RADSCAT

Direction	Pol.	Incidence angle		
		30°	40°	50°
Upwind	V	1.68	1.77	1.66
	H	1.65	1.98	1.93
Downwind	V	1.56	1.62	1.55
	H	1.68	1.97	1.96
Crosswind	V	1.49	1.52	1.51
	H	1.45	1.46	1.48

3.1.4. *Skylab S-193 RADSCAT data*

From Skylab, the S-193 RADSCAT measurements were frequently obtained at azimuths not aligned with or perpendicular to the surface wind, and because of the variable spacecraft attitude, NRCS measurements were not always obtained at the nominal incidence angles. Further, the surface backscatter was occasionally attenuated by clouds and rain. Because of these effects, the NRCS data were modified before being compared with the neutral-stability wind speed at 19.5 m. Young and Moore (1977) performed the corrections and transformed the measurements into upwind observations. They then used both nonlinear and linear regression analyses (Equations (1) and (2) respectively) to determine the wind-speed exponents. Data from the first two Skylab missions (SL2) and SL3) and the last mission (SL4) were analyzed separately because of antenna damage which changed the character of the measurements during SL4. Their results are summarized in Table VI for SL2 and SL3 only.

TABLE VI

Upwind wind-speed exponents for 13.9 GHz S-193 RADSCAT, SKYLAB 2 and 3

Pol.	Incidence angle		
	32°	43°	50°
V	1.39	1.89	1.69
H	1.32	1.89	1.81

3.2. NRCS VS FRICTION VELOCITY

When comparing the NRCS regression analyses for the NRL 4-FR and the 13.3-GHz data (e.g., Figures 1 and 2), one can conclude that either these measurements contain instrument biases (systematic on all four wavelengths for the 4-FR data) or that the ocean NRCS depends on variables other than the mean wind speed. Insight into this problem can be drawn from an examination of Bragg scattering theory which is generally accepted to be the primary mechanism for backscatter at incidence angles greater than approximately 25°.

Using small perturbation theory, Rice (1951) showed that radar scatterers are related to the radar wavelength, such that the radar return from adjacent crests of the most important ocean component add in phase. This leads to the Bragg condition:

$$\Lambda \sin \theta = n\lambda/2, \tag{3}$$

where Λ is the Bragg ocean-wavelength component, θ is the incidence angle, n is an integer, and λ is the radar wavelength.

For first-order scattering ($n = 1$) and an incidence angle of 30°, the Bragg wavelength for the ocean is the same as the probing radar wavelength. For radar frequencies of 8.9 and 13.3 GHz and incidence angles of 25 to 60°, the first-order Bragg wavelengths correspond to capillary wavelengths from 4 to 1.3 cm. Because the capillary spectrum grows monotonically with friction velocity U_* (Pierson and Stacy, 1973; Mitsuyasu and Honda, 1974), the NRCS should be a function of U_*.

The relationship of mean wind speed at some altitude to friction velocity is complex. In the model of Cardone (1970), the wind speed in the marine boundary layer follows a logarithmic profile which is itself a function of several variables in cluding the air-sea temperature difference and the mean wind speed. Therefore, it is reasonable to expect that the relationship between NRCS and mean wind speed is not unique.

With regards to the 'surface truth' used for the NRL 4-FR and 13.3-GHz data analyses, three factors become important. First, the wind speeds for each mission were not measured at the same altitude (anemometer heights ranged from approximately 10 to 41 m). Secondly, the reported wind speeds were not corrected for the effects of atmospheric stability (air-sea temperature difference). Finally, at the time that these experiments were performed, little was documented of the NRCS anisotropy (Jones *et al.*, 1977); therefore, there exists the possibility that the measured NRCS was not obtained at precisely the reported azimuth direction relative to the surface wind direction. The first and second factors could have contributed errors of several m s^{-1} in the specification of the 19.5-m neutral stability wind, and the third factor could have contributed errors of a few dB in the measured NRCS for moderate misalignements.

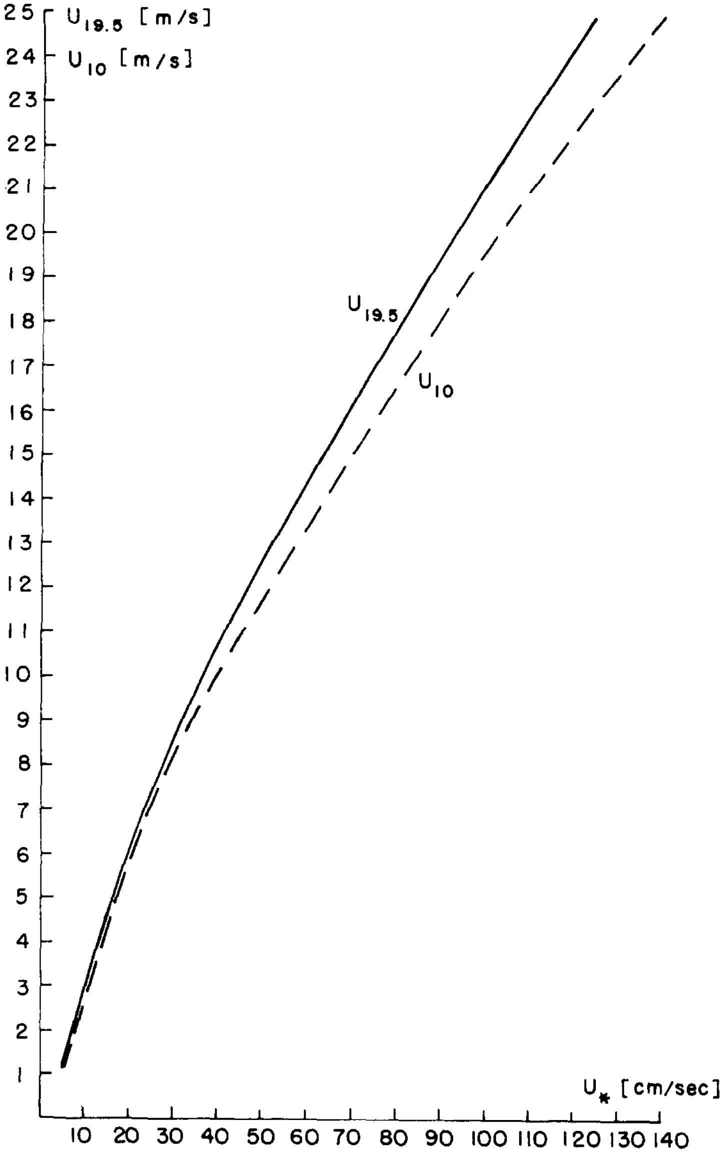

Fig. 3. $U_{10}(U_*)$ and $U_{19.5}(U_*)$ as a function of U_* in a neutrally stratified atmosphere (Cardone, 1970; Pierson and Stacy, 1973).

3.2.1. *NRCS vs* U_*

The values of U_* were obtained from the neutral stability 19.5-m wind using the method of Cardone (1970): the empirical relation employed is shown in Fig. 3. The AAFE RADSCAT data* were then reanalyzed using U_* in Equation (2) instead of U. A typical plot of the upwind NRCS vs U_* is shown for 40° incidence in Figure 4. Here the exponents are different than those for the 19.5-m neutral-stability wind-speed case, but the general trends with polarization, incidence angle, and radar azimuth relative to wind direction are the same. The results of this investigation, which are given in Table VII, show that to the first order, the NRCS for fixed incidence and azimuth angle can be modeled by a single ocean-surface variable U_* Admittedly this analyses does not consider additional variables such as fetch, current and water temperature. For fetch, however, the effects have been shown to be of second order (Ross and Jones, 1978).

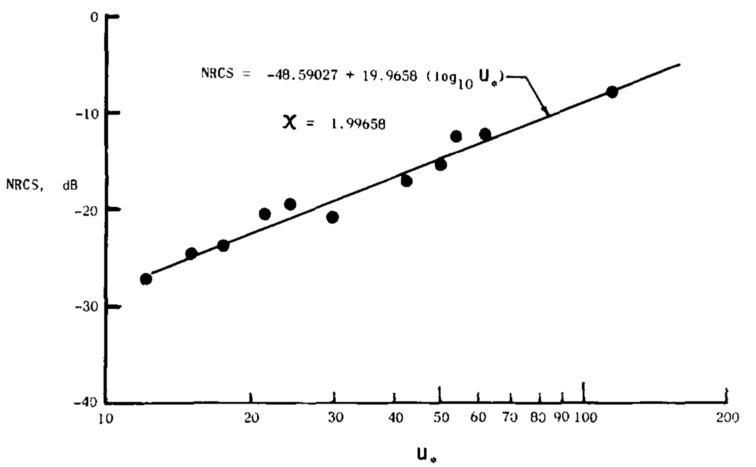

Fig. 4. Upwind, horizontal polarization, 13.9-GHz NRCS vs friction velocity, U_*, in cm s^{-1} for $\theta = 40°$.

TABLE VII

U_* *exponents for* 13.9 GHz AAFE RADSCAT

Direction	Pol.	30°	40°	50°
Upwind	V	1.73	1.93	1.93
	H	1.77	2.00	2.15
Downwind	V	1.55	1.68	1.65
	H	1.55	1.86	2.07
Crosswind	V	1.52	1.75	1.69
	H	1.49	1.80	1.90

* Additional unpublished NRCS measurements were included.

3.2.2. U_* Exponents vs Λ

To study the amplitude of short gravity and capillary waves as a function of U_*, the results of Section 3.1 were used. Even though the lack of air/sea temperature measurements make it impossible to convert the NRL 4-FR and the 13.3 GHz wind speeds to U_*, the wind-speed exponents were used to estimate the relative dependence of the U_* exponents with Λ. This appears to be justified from the results of the previous section. Further, concerning the NRL 4-FR and the 13.3 GHz data sets, we considered them from each individual mission to minimize the errors discussed at the beginning of this section. The wind-speed exponents for vertical polarization, upwind observation at a given radar frequency and incidence angle are plotted versus the corresponding Bragg wavelength in Figure 5. From these results, we deduce that the shorter wavelengths have increasingly larger amplitudes with increasing U_*. This conclusion is supported by the results of wave-tank measurements (Mitsuyasu and Honda, 1974) which show that the wave-number spectra spread farther apart with increasing wave number and grow more rapidly with U_* at high wave numbers than at low wave numbers. From this we further conclude that the NRCS measurements at the higher radar frequencies are more useful for remotely sensing U_*.

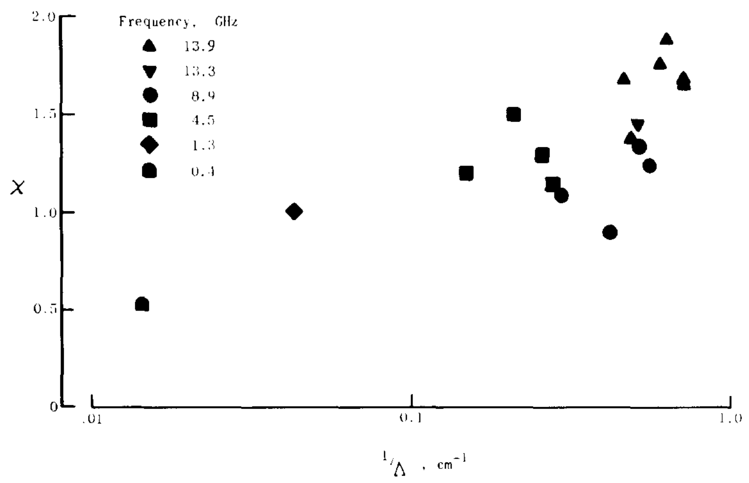

Fig. 5. Wind-speed exponent χ vs reciprocal Λ for upwind, vertical polarization.

3.3. NRCS ANISOTROPY

A directional dependence for NRCS has long been recognized by aircraft experimenters who have flown different patterns (upwind, etc.) to investigate this effect specifically. The most comprehensive measurements to date of the NRCS anisotropy have come from the AAFE RADSCAT experiments (Jones *et al.*, 1977).

These measurements showed the NRCS to be symmetric about the wind vector and to be expressed by the Fourier expansion:

$$\sigma^\circ(\theta, \phi) = \sum_m A_m(\theta) \cos m\phi, \ \phi m = 0, 1, 2\,, \tag{4}$$

where ϕ is the azimuth angle relative to the upwind direction (i.e.: $\phi = 0$ for upwind). The NRCS signature is predominantly secônd harmonic with a slight upwind/downwind assymetry. Typical signatures for vertical and horizontal polarizations are shown in Figure 6.

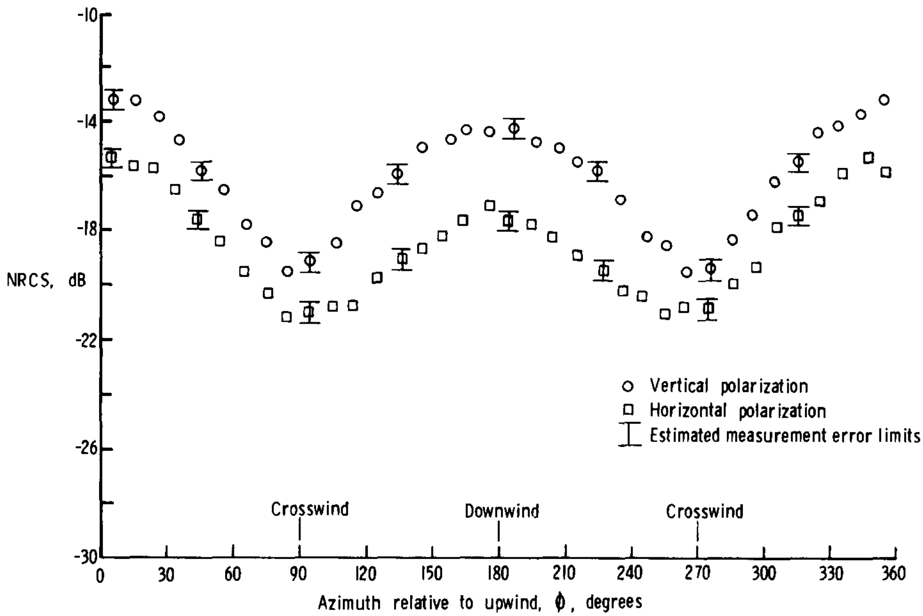

Fig. 6. Typical 13.9-GHz NRCS vs radar azimuth relative to upwind direction for 40° incidence angle. (AAFE RADSCAT Mission 318, Flight 17).

To examine the dependence of anisotropy on wind speed, Bragg wavelength, incidence angle and polarization, the following studies were conducted using the NRL 4-FR and the AAFE RADSCAT data.

3.3.1. *Wind Speed Dependence*

A linear regression analysis was performed using the NRL 4-FR (JOSS-1 and North Atlantic) and AAFE RADSCAT data at 30-deg incidence for vertical and horizontal polarization. The equation used was

$$\sigma^\circ_U/\sigma^\circ_i\,(\mathrm{dB}) = b(\mathrm{dB}) + y(10 \log U)\,, \tag{5}$$

where σ°_U is the upwind NRCS; σ°_i, $i = D$, is the downwind NRCS, $i = C$, is the crosswind NRCS; b is a constant; and y is the wind-speed exponent. The results of the analysis are given in Table VIII. The exponents are small and are both positive and negative with no apparent trend in frequency. Because of this randon distribution, we conclude that $\sigma_U^\circ/\sigma_D^\circ$ and $\sigma_U^\circ/\sigma_C^\circ$ are independent of wind speed.

TABLE VIII

Exponents of upwind-downwind and upwind/crosswind NRCS vs windspeed for 30° incidence angle

Direction	Pol.	Frequency, GHz				
		0.428	1.228	4.455	8.910	13.9
Upwind/downwind	V	−0.01	0.37	0.01	−0.17	−0.24
	H	0.36	0.29	0.31	−0.03	−0.28
Upwind/crosswind	V	0.70	0.60	−0.18	−0.57	−0.08
	H	0.45	0.67	0.34	−0.32	0.08

3.3.2. *Radar Parameters and Λ Dependence*

The dependence of the NRCS anisotropy on the Bragg wavelength, incidence angle, and polarization was studied using the NRL 4-FR data for 30 and 60° and the AAFE RADSCAT data for 30, 40 and 50°. The mean $\sigma_U^\circ/\sigma_D^\circ$ and $\sigma_U^\circ/\sigma_C^\circ$ computed from the above measurements were fit to an equation of the form

$$\sigma_U^\circ/\sigma_i^\circ(\text{dB}) = c(\text{dB}) + z(10\log 1/\Lambda), \tag{6}$$

where c is a constant expressed in dB and z is the exponent for the Bragg wavelength dependence.

For vertical polarization, results of the regression analyses were nearly the same (within statistical uncertainty) for the 30 and 60° data sets when used separately or combined. The $\sigma_U^\circ/\sigma_D^\circ$ was less than 1 dB and was nearly independent of Λ. On the other hand, the $\sigma_D^\circ/\sigma_C^\circ$ increased significantly with decreasing Λ. Therefore, for the capillary waves, the NRCS is highly anisotropic; whereas for the short gravity waves (approximately 100 cm in length), it is nearly isotropic. The $\sigma_U^\circ/\sigma_i^\circ$ are plotted vs reciprocal Λ in Figure 7 and the regression coefficients for the combined data are listed in Table IX

For horizontal polarization, the $\sigma_U^\circ/\sigma_D^\circ$ and the $\sigma_U^\circ/\sigma_C^\circ$ exponents z for the 30 and 60° data, respectively are nearly equal; however the c at 60° is approximately 1 dB greater for both $\sigma_U^\circ/\sigma_D^\circ$ and $\sigma_U^\circ/\sigma_C^\circ$ than the corresponding values at 30°. Thus for horizontal polarization, the NRCS anisotropy increases slightly with incidence angle as well as decreasing Bragg wavelength. The $\sigma_U^\circ/\sigma_i^\circ$ are plotted separately for 30 and 60° in Figure 8 (a) and (b) respectively, and the regression coefficients are also listed in Table IX.

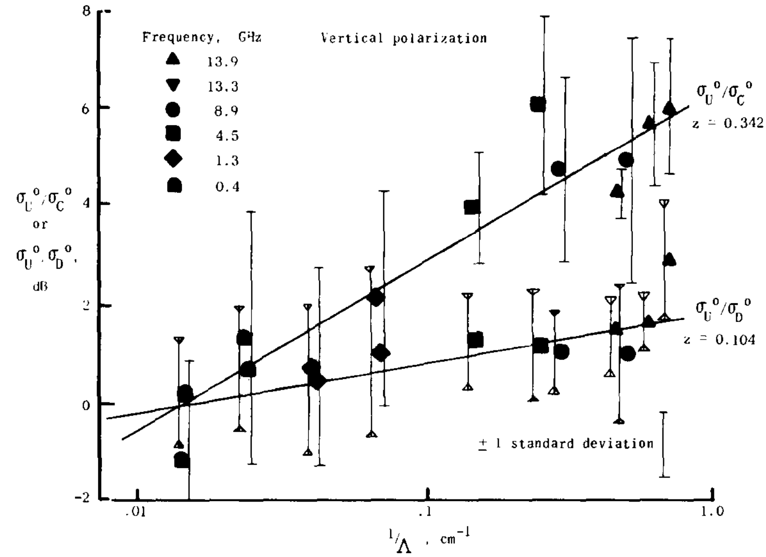

Fig. 7. Regression analysis; σ_U^0/σ_C^0 and σ_U^0/σ_D^0 vs reciprocal Bragg wavelength for vertical polarization.

TABLE IX

Upwind/downwind and upwind/crosswind NRCS regression against log of inverse Bragg wavelength

Direction	Pol.	Incidence angle	c	z
Upwind/downwind	V	30° and 60°	1.88	0.104
	H	30°	2.69	0.166
	H	60°	4.05	0.181
Upwind/crosswind	V	30° and 60°	6.47	0.342
	H	30°	5.42	0.342
	H	60°	6.28	0.304

4. Conclusions

From our analysis of ocean NRCS measurements for incidence angles between 30 and 60° and radar frequencies between 0.4 and 13.9 GHz we conclude:

(1) The NRCS is a function of the Bragg component Λ of the ocean-wave spectrum.

(2) For a given Λ between approximately 1 and 100 cm the NRCS is proportional to the friction velocity U_* raised to some power.

(3) The friction-velocity exponent is inversely proportional to Λ and varies approximately a factor of 3 over the Λ range of 1 to 100 cm.

(4) When Λ is in the capillary wave regime, the NRCS is highly anisotropic.

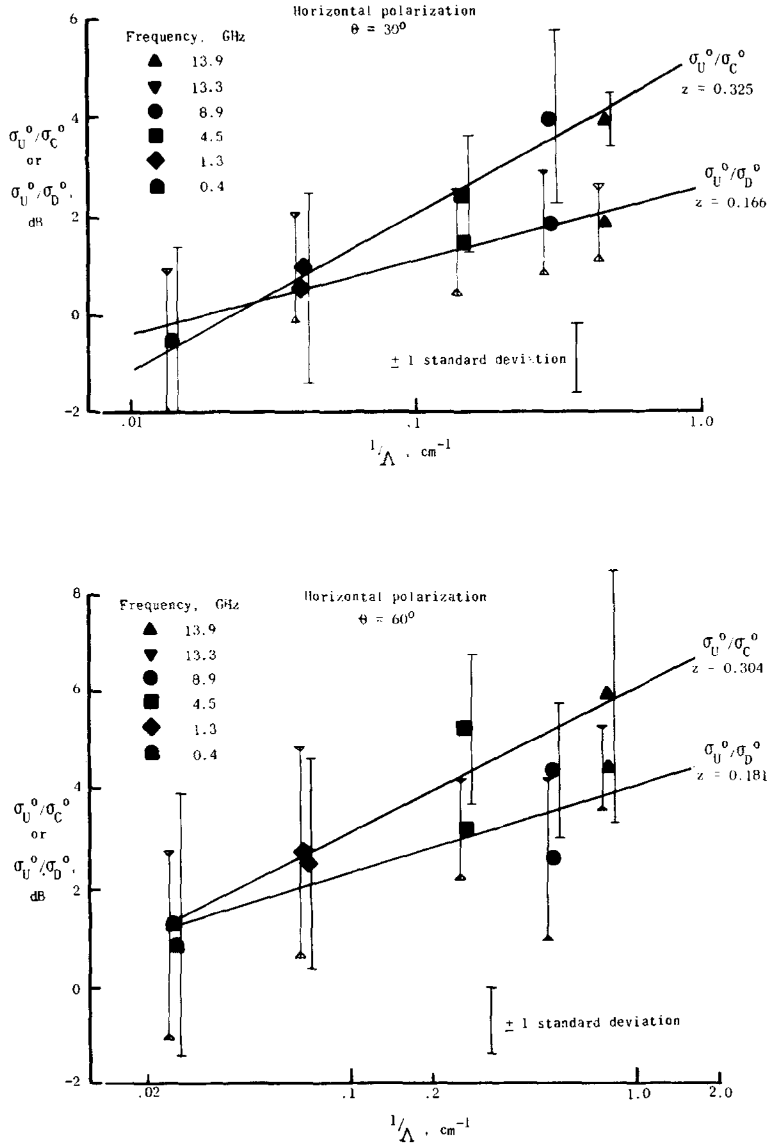

Fig. 8. Regression analysis: $\sigma_U^\circ/\sigma_C^\circ$ and $\sigma_U^\circ/\sigma_D^\circ$ vs reciprocal Bragg Wavelength for horizontal polarization. (a) $\theta = 30°$, (b) $\theta = 60°$.

(5) For a given Bragg wavelength, the NRCS anisotropy is similar for vertical and horizontal polarizations. The anisotropy is inversely proportional to Λ, and varies approximately by a factor of 6 for $\sigma_U^\circ/\sigma_C^\circ$ and 1.3 for $\sigma_U^\circ/\sigma_D^\circ$ over the Λ range of 1 to 100 cm. Further, the anisotropy is a weak function of incidence angle for horizontal polarization.

(6) For the radar data considered herein, the friction velocity (magnitude and direction) can best be inferred from Ku-band NRCS measurements at large incidence angles, with horizontal polarization slightly favored over vertical.

Acknowledgements

The authors wish to acknowledge the assistance of John L. Mitchell in data reduction and Aubrey E. Cross and Evelyn S. Martin in the preparation of the paper.

References

Bradley, G. A.: 1971, 'Remote Sensing of Ocean Winds using a Radar Scatterometer', Univ. of Kansas, Ph.D. Thesis, Lawrence, Ka., U.S.A.

Cardone, V. J.: 1970, 'Specifications of the Wind Distribution in the Marine Boundary Layer for Wave Forecasting', New York Univ. Report TR 69-1, Univ. Heights, N.Y., U.S.A.

Cardone, V. J., Young, J. D., Pierson, W. J., Moore, R. K., Greenwood, J. A., Greenwood, C., Fung, A. K., Salfi, R., Chan, H. L., Afarani, M., and Komen, M.: 1975, 'The Measurement of the Winds near the Ocean Surface with a Radiometer-Scatterometer on Skylab', NASA-JSC Contract NAS-9-13642 final report E-PN550, prepared jointly by CUNY and Univ. of Kansas CRES, Houston, Tex., U.S.A.

Claassen, J. P., Fung, A. K., Moore, R. K., and Pierson, W. J., Jr.: 1972, 'Radar Sea Return and the RADSCAT Satellite Anemometer', *IEEE Int. Conf. Engineering in the Ocean Environment*, Newport, R.I., U.S.A.

Claassen, J. P. and Fung, A. K.: 1972b, 'The Wind Response of NRL Scatterometric Observations at X-band', Univ. of Kansas, Center for Res. Tech Rep. 186-5, Lawrence, Kan., U.S.A.

Cowan, E. W.: 1946, 'X-band Sea-return Measurements', MIT Radiation Lab. Rep. 870, Cambridge, Mass., U.S.A.

Daley, J. C., Ransone, J. T., Jr., Burkett, J. A., and Duncan, J. R.: 1968, 'Sea-Clutter Measurements on Four Frequencies', U.S. Naval Res. Lab. Rep. 6806, Wash., D.C., U.S.A.

Daley, J. C., Davis, W. T., and Mills, N. R.: 1970, 'Radar Sea Return in High Sea States', U.S. Naval Res. Lab. Rep. 7142, Wash., D.C., U.S.A.

Daley, J. C., Ransone, J. T., Jr., and Burkett, J. A.: 1971, 'Radar Sea Return-JOSS I', U.S. Naval Res. Lab. Rep. 7268, Wash., D.C., U.S.A.

Daley, J. C., Ransone, J. T., Jr., and Davis, W. T.: 1973, 'Radar Sea Return-JOSS II', U.S. Naval Res. Lab. Rep. 7534, Wash., D.C., U.S.A.

Daley, J. C.: 1973b, 'An Empirical Sea Clutter Model', U.S. Naval Res. Lab. Rep. 2668, Wash., D.C., U.S.A.

Daley, J. C.: 1973c, 'Wind Dependence of Radar Sea Return', *J. Geophys. Res.* **78**, 7823.

Daley, J. C.: 1974, 'Reply', *J. Geophys. Res.* **79**, 2756.

Grant, C. R. and Yapley, B. S.: 1957, 'Backscattering from Water and Land at Centimeter and Millimeter Wavelengths', *Proc. IRE* **45**, 976.

Guinard, N. W., Ransone, J. T., Jr., and Daley, J. C.: 1971, 'Variation of the NRCS of the Sea with Increasing Roughness', *J. Geophys. Res.* **76**, 1525.

Jackson, F. C.: 1974, 'Comment on Wind Dependence of Radar Sea Return by J. C. Daley, *J. Geophys. Res.* **79**, No. 18.

Jones, W. L., Schroeder, L. C., and Mitchell, J. L.: 1977, 'Aircraft Measurements of the Microwave Scattering Signature of the Ocean', *IEEE J. Oceanic Eng.* **OE-2**, 52.

Kerr, D. E.: 1951, 'Propagation of Short Radio Waves', M.I.T. Radiation Lab. Ser., Chapter 6, McGraw-Hill, N.Y., U.S.A.

Krishen, K.: 1971, 'Correlation of Radar Backscattering Cross Sections with Ocean Wave Height and Wind Velocity', *J. Geophys. Res.* **76**, 6528.

Mitsuyasu, H. and Honda, T.: 1974, 'The High Frequency Spectrum of Wind Generated Waves', *J. Oceanograph. Soc. Japan* **30**, 185.

Newton, R. W. and Rouse, J. W., Jr.: 1972, 'Experimental Measurements of 2.25-cm Backscatter from Sea Surfaces', *IEEE-Trans. Geosci. Electron.* **GE-10**, 2.

Pierson, W. J. and Stacy, R. A.: 1973, 'The Elevation Slope, and Curvature Spectra of a Wind Roughened Sea Surface', NASA CR-2247, Wash. D.C., U.S.A.

Rice, S. O.: 1951, 'Reflection of Electromagnetic Waves from Slightly Rough Surfaces', *Comm. Pure Appl. Math.* **4**, 351.

Ross, D. and Jones, W. L.: 1978, 'On the Relationship of Radar Backscatter to Windspeed and Fetch', this volume, pp. 151–163.

Sittrop, H.: 1974, 'X- and k_u-band Radar Backscatter Characteristics of Sea-clutter', Pro. URSI Specialist Meeting on Microwave Scattering and Emission from the Earth, Berne, Switzerland.

Young, J. D. and Moore, R. K.: 1977, 'Active Microwave Measurements from Space of Sea-Surface Winds', *IEEE J. Oceanic Eng.* **OE 2**, No. 4.